Sustainability in Environment
ISSN 2470-637X (Print) ISSN 2470-6388 (Online)
Vol. 8, No. 4, 2023
www.scholink.org/ojs/index.php/se

Original Paper

Semi-analytical Modeling of Fractured Horizontal Wells in Heterogeneous Formations Considering the Interference between Hydraulic Fractures

Fangdong Zhou[1], Yanwen Yu[2], Pinlu Cao[1], Liangliang Jiang[3], Shanshan Yao[1*]

[1] College of Construction Engineering, Jilin University, China

[2] Research Institute of Petroleum Exploration and Development, China

[3] College of Chemical and Petroleum Engineering, University of Calgary, Canada

Received: August 27, 2023 Accepted: November 11, 2023 Online Published: November 24, 2023

doi:10.22158/se.v8n4p92 URL: http://dx.doi.org/10.22158/se.v8n4p92

Abstract

In this study, a semi-analytical model is developed for the pressure and rate transient analysis of multi-stage fractured horizontal wells. This model simulates the fluid flow towards a fractured horizontal well centered in an unconventional formation with considering the interferences between hydraulic fractures under various heterogeneity conditions. In this proposed model, the formation is divided into sub-systems, and each sub-system is further composed of linear flow regions. Boundaries of the linear flow regions are being updated in real-time response to the interferences between hydraulic fractures. Applicability of the proposed model in heterogeneous reservoirs is demonstrated by the comparison with the five-region model published in literature. The proposed model is applicable to the heterogeneity conditions including a fractured horizontal well having heterogeneous completions and/or the formation being heterogeneous in reservoir properties. Furthermore, the proposed model is utilized to analyze field data from fractured horizontal wells in heterogeneous conditions.

Keywords

heterogeneity, linear flow, hydraulic fractures, unconventional reservoirs, pressure and rate transient analysis

1. Introduction

Effective hydrocarbon production of low-permeability unconventional formations (e.g., tight sandstone reservoirs, shale formations) currently relies on horizontal well drilling coupled with multi-stage hydraulic fracturing operations (Figure. 1). Multiple fractures are created along the horizontal wellbore,

providing high-conductivity channels for the flow of oil and/or gas and increasing the contact area with formations (Denney, 2010; King, 2014). The horizontal wellbore and multiple hydraulic fractures in the target formation constitute a complex flow system, mainly composed of the fluid flow in the surrounding formation, the fluid flow within hydraulic fractures, and the fluid flow along the wellbore. Multi-stage fractured horizontal wells have wellbore lengths typically ranging from 1000 m to 3000 m as well as 10 to 40 stages of hydraulic fractures (Yuan, 2023; Wei et al., 2015; Grieser et al., 2009; Song et al., 2011). Therefore, the productivity of a horizontal well is affected by characteristics of the well including the wellbore length, hydraulic fracture conductivities, and number of fracture stages as well as reservoir properties such as including porosity, permeability, rock compressibility, and natural fractures, etc. (Zawila et al., 2015). Many of the low-permeability unconventional formations where multi-stage hydraulic fracturing operations are generally utilized exhibit heterogeneity in reservoir properties. Deng et al. (2023) investigated the heterogeneity of an oil shale formation located in Weixinan, Beibu Gulf Basin, China. Table 1 provides the porosity and permeability data measured on the shale and tight sandstone samples retrieved from Weixinan, Beibu Gulf Basin. Rock porosity varies significantly from 2.6% to 16.7% due to strong heterogeneity and correspondingly, rock permeability varies in a wide range of (0.01 mD, 2.75 mD).

Table 1. Porosities and Permeabilities Measured on the Shale and Sandstone Samples from Weixinan Sag, Beibu Gulf Basin of China (Deng et al., 2023).

Lithofacies	Porosity, %	Permeability, mD
Silica-rich clayey shale	2.6 ~ 16.2	0.12 ~ 1.58
Mixed mud shale	2.9 ~ 4.9	0.11 ~ 0.80
Clay-rich silty siltstone	4.7 ~ 11.9	0.01 ~ 1.73
Siliceous sandstone	8.0 ~ 16.7	0.04 ~ 2.75

Numerical simulations of multiple fractured horizontal wells in low-permeability reservoirs are flexible in modeling complex heterogeneity (Xie et al., 2022; Freeman et al., 2013; Ren et al., 2014). For instance, in the numerical models of Yue et al. (2013), heterogeneity of natural fractures had been considered into their simulations of a fractured horizontal well's production behavior. Their results suggested that for a given quantity of natural fractures, the fractured horizontal well exhibits lower productions when the natural fractures are heterogeneously distributed as compared against the condition of natural fractures being uniformly distributed. However, incorporating heterogeneity into numerical simulations of multi-stage fractured horizontal wells increases computational costs and raises the possibility such as non-convergence and significant computational errors. These greatly limit the applicability of numerical simulations in real-time monitoring and quick production analysis (Seales, 2020). Semi-analytical modeling technique which integrates the advantages of analytical models and numerical simulations can offer production modeling at enough accuracy but with less computational cost and strong applicability to complex reservoir conditions (Ning et al., 2020; Yao et al., 2013). Various semi-analytical models of

fractured horizontal wells based on linear flow modeling have built extensive applications in the reservoir engineering and formation evaluation of unconventional reservoirs (Yao et al., 2020; Wang et al. 2015; Yuan et al., 2015). Production of the unconventional formations stimulated by multi-stage fractured horizontal wells usually exhibits extended periods of formation linear flow (Figure 1). Streamlines of the formation linear flow are perpendicular to the orientation of hydraulic fractures (Nobakht et al., 2012). In 1981, Cinco-Ley and Samaniego-V (1981) combined the modeling of formation linear flow with hydraulic fracture linear flow to form a bi-linear flow model for fractured vertical wells. Lee and Brockenbrough (1986) extended the bi-linear model to a tri-linear model for fractured vertical wells. The tri-linear model couples the linear flow in an inner formation, the linear flow in an outer formation, as well as the linear flow through hydraulic fractures. Brown et al. (2011) applied the tri-linear scheme in the modeling of multi-stage fractured horizontal wells based on the assumption that all the hydraulic fractures along a horizontal wellbore are identical. In the tri-linear model, inner formation could own reservoir properties different from the outer formation. Later five-region model and seven-region model are proposed by Stalgorova et al. (2013) and Zeng et al. (2018), respectively. Five-region and seven-region models can be utilized when the formations in the vicinity of hydraulic fractures exhibit permeabilities and porosities different from the far-away regions. Yao et al. (2020) developed a semi-analytical composite model of fractured horizontal wells in heterogeneous reservoir with combing the formation linear flow, hydraulic fracture linear flow, radial flow, and source-sink flow. Although extensively utilized in production data analysis, these semi-analytical models of fractured horizontal wells on the basis of linear flow modeling ignore the mutual interferences between fractured fractures spaced along a horizontal wellbore. It limits the computation accuracy of these linear-flow-based semi-analytical models in heterogeneous conditions, especially the heterogeneity along the extension of horizontal wellbores.

Characterizing the interferences between fractured fractures is crucial for quick-and-accurate assessment on the production of multi-stage fractured horizontal wells under various heterogeneous conditions. In this study, based on the modeling of linear flows, we develop a semi-analytical model by dividing formation into many linear flow regions. Boundaries of the linear flow regions are being updated in real-time response to the interferences between hydraulic fractures. The proposed model calculates the variation of bottomhole flowing pressure vs. time for fractured horizontal wells under different heterogeneous conditions.

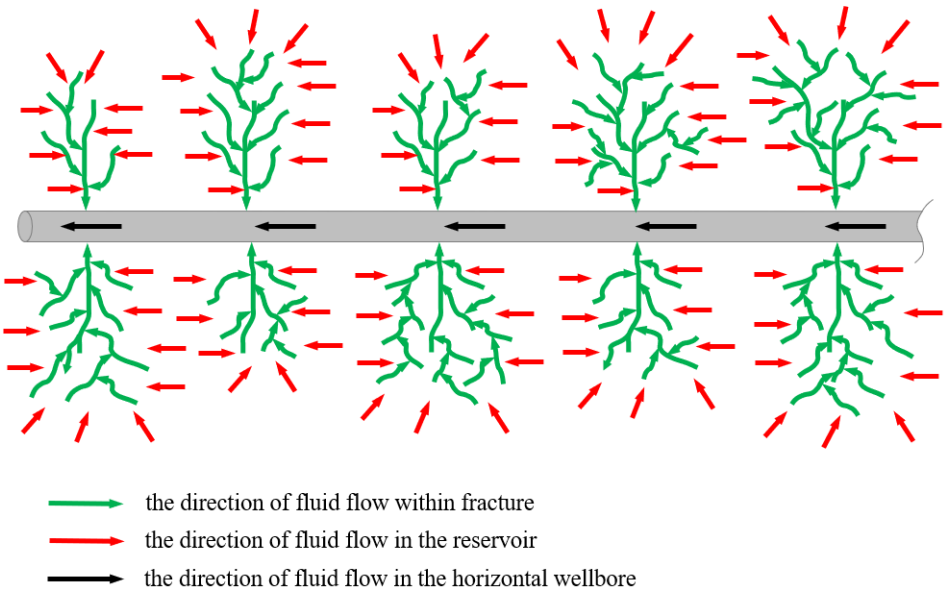

Figure 1. A 2D Schematic of an Unconventional Formation Stimulated with a Multi-stage Fractured Horizontal Well.

2. Mathematical Modeling

This study establishes a semi-analytical model of fractured horizontal wells under the following assumptions:

(1) A multi -stage fractured horizontal well is located in the central of a formation with four closed boundaries. The two boundaries that are aligned with the horizontal wellbore define a no-flow condition between adjacent horizontal wells.

(2) Each hydraulic fracture is vertically symmetrical with regards to the horizontal wellbore and completely penetrates the target formation.

(3) The fluid flow within formations and through hydraulic fractures are treated as single-phase flow.

(4) Pressure loss due to the pipe flow along the horizontal wellbore is neglected.

Table 2 summarizes definitions for all the dimensionless variables in the proposed semi-analytical model. Values of the reference variables in Table 2, including reference permeability k_{ref}, reference rate q_{ref}, reference pressure p_{ref}, reference porosity ϕ_{ref}, reference total compressibility c_{tref}, and reference length L_{ref} can be selected by users. Table 2 further lists values of the reference variables chosen for this study.

Table 2. Definition of Dimensionless Variables and Values of Reference Variables in the Proposed Model.

Dimensionless pressure p_D	$p_D = \begin{cases} \frac{2\pi k_{ref} H}{q_{ref} B_o \mu}(p_i - p), & \text{for oil} \\ \frac{\pi k_{ref} H}{q_{ref} B_g p_{ref}}\left(m(p_i) - m(p)\right) & \text{for gas} \end{cases}$	(1)
Dimensionless time t_D	$t_D = \frac{\eta_{ref} t}{L_{ref}^2}, \eta_{ref} = \frac{k_{ref}}{\phi_{ref} \mu C_{tref}}$	(2)
Dimensionless distance x_D	$x_D = \frac{x}{L_{ref}}, y_D = \frac{y}{L_{ref}}, w_{fD} = \frac{w_f}{L_{ref}}$	(3)
Dimensionless diffusivity η_D	$\eta_D = (\frac{k}{\phi \mu C_t})/\eta_{ref}$	(4)
Dimensionless fracture conductivity F_{CD}	$F_{CD} = \frac{w_f k_f}{L_{ref} k_{ref}}$	(5)
Dimensionless rate q_D	$q_D = \frac{q}{q_{ref}}$	(6)
Dimensionless permeability k_D	$k_D = \frac{k}{k_{ref}}$	(7)
Pseudo-pressure $m(p)$	$m(p) = 2\int_{p_{ref}}^{p} \frac{p}{\mu(p) z(p)} dp$	(8)
Reference permeability k_{ref}	1 mD	
Reference rate q_{ref}	0.0002 m^3/s	
Reference pressure p_{ref}	1.01×10^5 Pa	
Reference porosity ϕ_{ref}	0.1	
Reference compressibility C_{tref}	1.45×10^{-10} Pa^{-1}	
Reference length L_{ref}	30 m	

When compared against fractured vertical wells, the production of multi-stage fractured horizontal wells usually exhibits extended formation linear flow regime. Streamlines of linear flow in formations are parallel to each other. Based on the linear flows, the formation stimulated with a multi-stage fractured horizontal well can be divided into sub-systems based on the number of fracturing stages. Each sub-system represents a part of the formation influenced by a hydraulic fracture during production. A sub-system is further composed of multiple linear flow regions. Figure 2 shows a combination of linear flow regions built for a horizontal well stimulated with four-stage hydraulic fractures. The formation is first divided into four sub-systems and each sub-system encloses one hydraulic fracture. Fluid flow inside a hydraulic fracture is linear flow. There exist linear flow regions both on the left-hand and right-hand sides of each hydraulic fracture. As illustrated in Figure 2, this study classifies three types of linear flow regions: (*x*-direction) formation linear flow region, *y*-direction linear flow region, and fracture linear region. Regions of *y*-direction linear flow represents the part of the formation beyond hydraulic fracture tips, while regions of *x*-direction linear flow have streamlines perpendicular to hydraulic fracture planes.

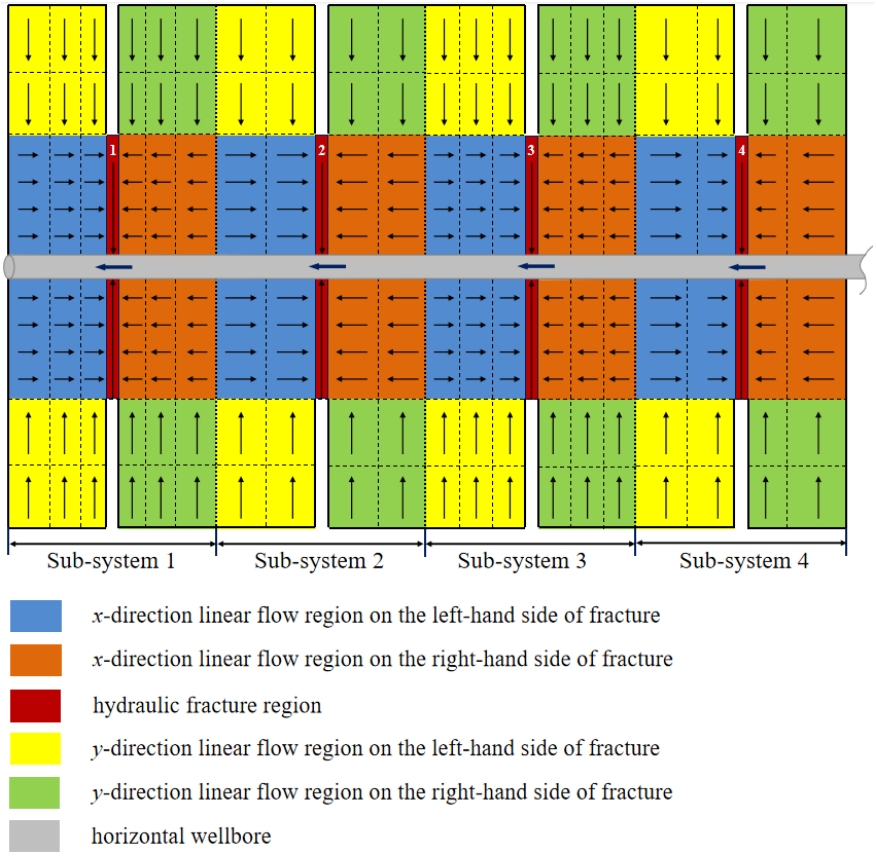

Figure 2. An Example of Sub-systems and Linear Flow Regions for a Horizontal Well Stimulated with Four-stage Hydraulic Fractures. Black Arrow Indicates the Direction of Fluid Flow.

2.1 Coupling of Linear Flow Regions

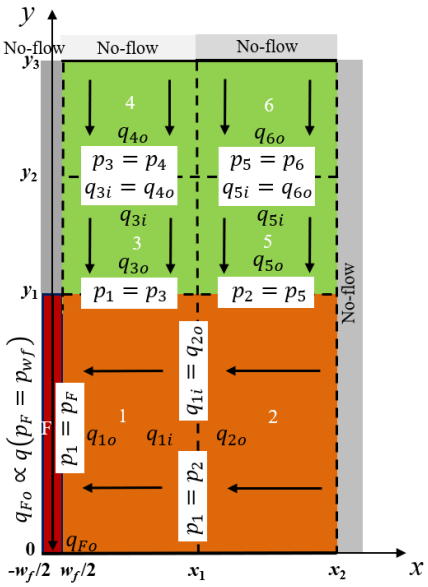

Figure 3. Fluid Flow Directions and Boundary Conditions for the Example Linear Flow Regions.

Governing equations of linear flow in each of the flow regions are keys to the development of our semi-analytical model. We take the linear flow regions on the upper-right side of the second hydraulic fracture for an example (Figure 3) to illustrate the procedure of development our semi-analytical model. In our model, the real time domain is first discretized into *n* time steps $t = t_{Di}$, *i*=1, 2, 3…*n*. During a given period of (t_{Di}, t_{Di+1}), the governing equation in Laplace domain for the linear flow in No.1 *x*-direction linear flow region becomes

$$\frac{\partial^2 \bar{p}_{1D}}{\partial x_D^2} + \frac{k_3}{k_1 y_{1D}} \frac{\partial^2 \bar{p}_{3D}}{\partial y_D^2}|_{y_{1D}} - \frac{s}{\eta_{1D}} \bar{p}_{1D} = -\frac{p_{1D}(\Delta t_D=0)}{\eta_{1D}}, \quad (9)$$

where k_1 is the permeability of this No. 1 region, k_3 is the permeability of this No. 3 region, *s* is Laplace variable corresponding to the real time variable $\Delta t_D = t_{Di+1} - t_{Di}$, $\bar{p}_D$ represents the dimensionless fluid pressure in the Laplace domain, and $\frac{k_3}{k_1 y_{1D}} \frac{\partial^2 \bar{p}_{3D}}{\partial y_D^2}|_{y_{1D}}$ describes the flow rate continuity at the interface between No.1 region and its adjacent No. 3 region. At the start of this period, i.e., $\Delta t_D = 0$, the initial pressure distribution in a small-enough linear flow region can be simplified as a linear expression of location x_D with two coefficients a_1 and b_1:

$$p_{1D}(\Delta t_D = 0, t_D = t_{Di+1} - \Delta t_D) = a_1 x_D + b_1, \quad (10a)$$

This No. 1 *x*-direction linear flow region shares a boundary with No. 2 linear flow region with following both pressure and rate continuity

$$\bar{p}_{1D}(x_{1D}) = \bar{p}_{2D}(x_{1D}), \quad (10b)$$

$$\frac{k_2}{\mu} \frac{\partial^2 \bar{p}_{2D}}{\partial x_D^2}|_{x_{1D}} = \frac{k_1}{\mu} \frac{\partial^2 \bar{p}_{1D}}{\partial x_D^2}|_{x_{1D}}, \quad (10c)$$

where k_2 is the permeability of this No. 2 region. Similarly, the boundary condition at the interface between No. 1 region and the fracture linear flow region can be written as

$$\bar{p}_{1D}(\frac{w_{fD}}{2}, \frac{y_{1D}}{2}) = \bar{p}_{FD}(\frac{w_{fD}}{2}, \frac{y_{1D}}{2}), \quad (10d)$$

where w_{fD} is dimensionless fracture width and y_{1D} is dimensionless fracture half-length for the hydraulic fracture shown in Figure 3. Solution to Eq. (9) is obtained

$$\bar{p}_{1D}(x_D) = A_{x1} \cosh\left[(x_D - x_{1D})\sqrt{\frac{s}{\eta_{1D}}}\right] + B_{x1} \sinh\left[(x_D - x_{1D})\sqrt{\frac{s}{\eta_{1D}}}\right] + \frac{a_1}{s} x_D + \frac{b_1}{s} + \frac{1}{y_{1D}\frac{s}{\eta_{1D}}} \frac{\partial \bar{p}_{1D}}{\partial y_D}|_{y_{1D}}, \quad (11)$$

A_{x1} and B_{x1} can be determined based on the initial and boundary conditions listed as Eqs. (10a-10d). During the given period of (t_{Di}, t_{Di+1}), the governing equation and associated initial and boundary conditions for the linear flow in No. 2 *x*-direction linear flow region are given by

$$\frac{\partial^2 \bar{p}_{2D}}{\partial x_D^2} + \frac{k_5}{k_2 y_{1D}} \frac{\partial^2 \bar{p}_{5D}}{\partial y_D^2}|_{y_{1D}} - \frac{s}{\eta_{2D}} \bar{p}_{2D} = -\frac{p_{2D}(\Delta t_D=0)}{\eta_{2D}}, \quad (12)$$

$$p_{2D}(\Delta t_D = 0, t_D = t_{Di+1} - \Delta t_D) = a_2 x_D + b_2, \quad (13a)$$

$$\frac{\partial^2 \bar{p}_{2D}}{\partial x_D^2}|_{x_{2D}} = 0 \text{ for the no-flow boundary,} \quad (13b)$$

$$\bar{p}_{1D}(x_{1D}) = \bar{p}_{2D}(x_{1D}), \tag{13c}$$

$$\frac{k_2}{\mu}\frac{\partial^2 \bar{p}_{2D}}{\partial x_D^2}|_{x_{1D}} = \frac{k_1}{\mu}\frac{\partial^2 \bar{p}_{1D}}{\partial x_D^2}|_{x_{1D}}, \tag{13d}$$

where k_5 is the permeability of No. 5 *y*-direction linear flow region. Solution to Eq. (12) becomes

$$\bar{p}_{2D}(x_D) = A_{x2}\cosh\left[(x_D - x_{2D})\sqrt{\frac{s}{\eta_{2D}}}\right] + B_{x2}\sinh\left[(x_D - x_{2D})\sqrt{\frac{s}{\eta_{2D}}}\right] + \frac{a_2}{s}x_D + \frac{b_2}{s} +$$

$$\frac{k_5}{k_2 y_{1D}\frac{s}{\eta_{2D}}}\frac{\partial \bar{p}_{5D}}{\partial y_D}|_{y_{1D}}, \tag{14}$$

Similarly, A_{x2} and B_{x2} can be determined based on the initial and boundary conditions shown in Eqs. (13a-13d).

During the given period of (t_{Di}, t_{Di+1}), the governing equation in Laplace domain for the linear flow in No. 3 *y*-direction linear flow region is

$$\frac{\partial^2 \bar{p}_{3D}}{\partial y_D^2} - \frac{s}{\eta_{3D}}\bar{p}_{3D} = -\frac{p_{3D}(\Delta t_D = 0)}{\eta_{3D}}, \tag{15}$$

with the initial pressure condition as

$$p_{3D}(\Delta t_D = 0, t_D = t_{Di+1} - \Delta t_D) = a_3 y_D + b_3, \tag{16a}$$

and the pressure and flow rate continuity condition at the interface between this No. 3 region and No. 4 region as

$$\frac{k_4}{\mu}\frac{\partial^2 \bar{p}_{4D}}{\partial y_D^2}|_{y_{2D}} = \frac{k_3}{\mu}\frac{\partial^2 \bar{p}_{3D}}{\partial y_D^2}|_{y_{2D}}, \tag{16b}$$

$$\bar{p}_{3D}(y_{2D}) = \bar{p}_{4D}(y_{2D}), \tag{16c}$$

where k_4 is the permeability of No. 4 region and the boundary condition at the interface between No. 3 region and No. 1 region can be written as

$$\bar{p}_{3D}(y_{1D}, \frac{x_{1D}}{2}) = \bar{p}_{1D}(y_{1D}, \frac{x_{1D}}{2}), \tag{16d}$$

Solution to Eq. (15) is written as

$$\bar{p}_{3D}(y_D) = A_{y3}\cosh\left[(y_D - y_{2D})\sqrt{\frac{s}{\eta_{3D}}}\right] + B_{y3}\sinh\left[(y_D - y_{2D})\sqrt{\frac{s}{\eta_{3D}}}\right] + \frac{a_3}{s}y_D + \frac{b_3}{s}, \tag{17}$$

A_{y3} and B_{y3} can be determined based on the initial and boundary conditions shown in Eqs. (16a-16d). Governing equation, initial conditions, and boundary conditions for No. 5 *y*-direction linear flow region can be written in the same format as No. 3 region.

During the given period of (t_{Di}, t_{Di+1}), the governing equation in Laplace domain for No. 4 *y*-direction linear flow region becomes

$$\frac{\partial^2 \bar{p}_{4D}}{\partial y_D^2} - \frac{s}{\eta_{4D}}\bar{p}_{4D} = -\frac{p_{4D}(\Delta t_D = 0)}{\eta_{4D}}, \tag{18}$$

The initial pressure condition for No. 4 region is given as

$$p_{4D}(\Delta t_D = 0, t_D = t_{Di+1} - \Delta t_D) = a_4 y_D + b_4, \tag{19a}$$

In addition to the pressure and flow rate continuity conditions between No. 3 region and No. 4 region, the linear flow in this No. 4 region is also constrained by a no-flow boundary at $y = y_{3D}$

$$\frac{\partial^2 \bar{p}_{4D}}{\partial y_D^2}|_{y_{3D}} = 0, \tag{19b}$$

Solution to Eq. (18) is written as

$$\bar{p}_{4D}(y_D) = A_{y4}\cosh\left[(y_D - y_{3D})\sqrt{\frac{s}{\eta_{4D}}}\right] + B_{y4}\sinh\left[(y_D - y_{3D})\sqrt{\frac{s}{\eta_{4D}}}\right] + \frac{a_4}{s}y_D + \frac{b_4}{s}, \tag{20}$$

A_{y4} and B_{y4} can be determined based on the initial and boundary conditions shown in Eqs. (16b-16c) and Eqs. (19a-19b). Governing equation, initial conditions, and boundary conditions for No. 6 *y*-direction linear flow region can be written in the same format as No. 4 region.

Governing equation for the fracture linear flow region is given by

$$\frac{\partial^2 \bar{p}_{FD}}{\partial y_D^2} - \frac{s}{\eta_{FD}}\bar{p}_{FD} + \frac{1}{w_{fD}}\left(\frac{\partial \bar{p}_{FD}}{\partial x_D}|_{x_D=\frac{w_{fD}}{2}} - \frac{\partial \bar{p}_{FD}}{\partial x_D}|_{x_D=\frac{-w_{fD}}{2}}\right) = -\frac{p_{FD}(\Delta t_D=0)}{\eta_{FD}}, \tag{21}$$

with its initial condition

$$p_{FD}(\Delta t_D = 0, t_D = t_{Di+1} - \Delta t_D) = a_F y_D + b_F, \tag{22a}$$

In addition to the flow rate continuity condition with regards to No. 1 region, the pressure continuity condition at the intersection between fracture and wellbore can be written as

$$\bar{p}_{wfD} = \bar{p}_{FD}(y_D = 0), \tag{22b}$$

and no-flow condition beyond the fracture tip can be written as

$$\frac{\partial^2 \bar{p}_{FD}}{\partial y_D^2}|_{y_{1D}} = 0 \text{ for the no-flow boundary,} \tag{22c}$$

where $\bar{p}_{wfD}$ represents the dimensionless bottomhole flowing pressure in Laplace domain. Solution to Eq. (21) is written as

$$\bar{p}_{FD}(y_D) = A_F\cosh\left[(y_D - y_{1D})\sqrt{\frac{s}{\eta_{FD}}}\right] + B_F\sinh\left[(y_D - y_{1D})\sqrt{\frac{s}{\eta_{FD}}}\right] + \frac{a_F}{s}y_D + \frac{b_F}{s}$$

$$+\frac{1}{w_{fD}}\left(\frac{\partial \bar{p}_{FD}}{\partial x_D}|_{\frac{w_{fD}}{2}} - \frac{\partial \bar{p}_{FD}}{\partial x_D}|_{\frac{-w_{fD}}{2}}\right)/\frac{s}{\eta_{FD}}, \tag{23}$$

A_F and B_F can be determined based on the initial and continuity conditions shown in Eqs. (22a-22c).

2.2 Coupling of Sub-systems

Since pressure drop along the horizontal wellbore is neglected, all the hydraulic fractures share the same pressure at the fracture-wellbore intersections:

$$\bar{p}_{1FD}(y_{0D}) = \bar{p}_{2FD}(y_{0D}) = \cdots = \bar{p}_{nFD}(y_{0D}), \tag{24}$$

where $\bar{p}_{iFD}$ comes from the *i*-th hydraulic fracture in *i*-th sub-system. If this *n*-stage fractured horizontal well produces at a constant rate *q*, the sum of the production rates from all the hydraulic fractures satisfies:

$$\sum_{i=1}^{n}\bar{q}_{iFD} = \bar{q}_D, i = 1, 2, 3 \ldots n, \tag{25}$$

where $\bar{q}_{iFD}$ represents the rate contribution made by i-th hydraulic fracture. If this n-stage fractured horizontal well produces at a constant flowing bottomhole pressure p_{wf}, the pressure at the fracture-wellbore intersection within each subsystem satisfies

$$\bar{p}_{wfD} = \bar{p}_{iFD}(y_{0D}), i = 1, 2, 3 \ldots n, \quad (26)$$

Interface between adjacent sub-systems defines the extent of the formation controlled by the hydraulic fractures enclosed in the sub-systems. During the production of a multi-stage fractured horizontal well, the interference among hydraulic fractures may lead to expansion or contraction of the flow regions influenced by the hydraulic fractures. Most of the linear-flow-based semi-analytical models cannot equip flow regions with movable boundaries due to the underlying fixed-boundary assumption. In this study the boundary between any two adjacent sub-systems, i.e., the boundary between any two flow regions which are adjacent to each other but belong to distinct sub-systems, is allowed to move during production. Direction and distance of the boundary movement can be determined from the difference between the pressures of flow regions at this shared boundary. A pressure difference threshold Δp_{max}, is set in this semi-analytical model. As shown in Figure 4, for each boundary between sub-systems, its location needs to be updated during each time step in order to keep the pressure difference at this boundary below the threshold value.

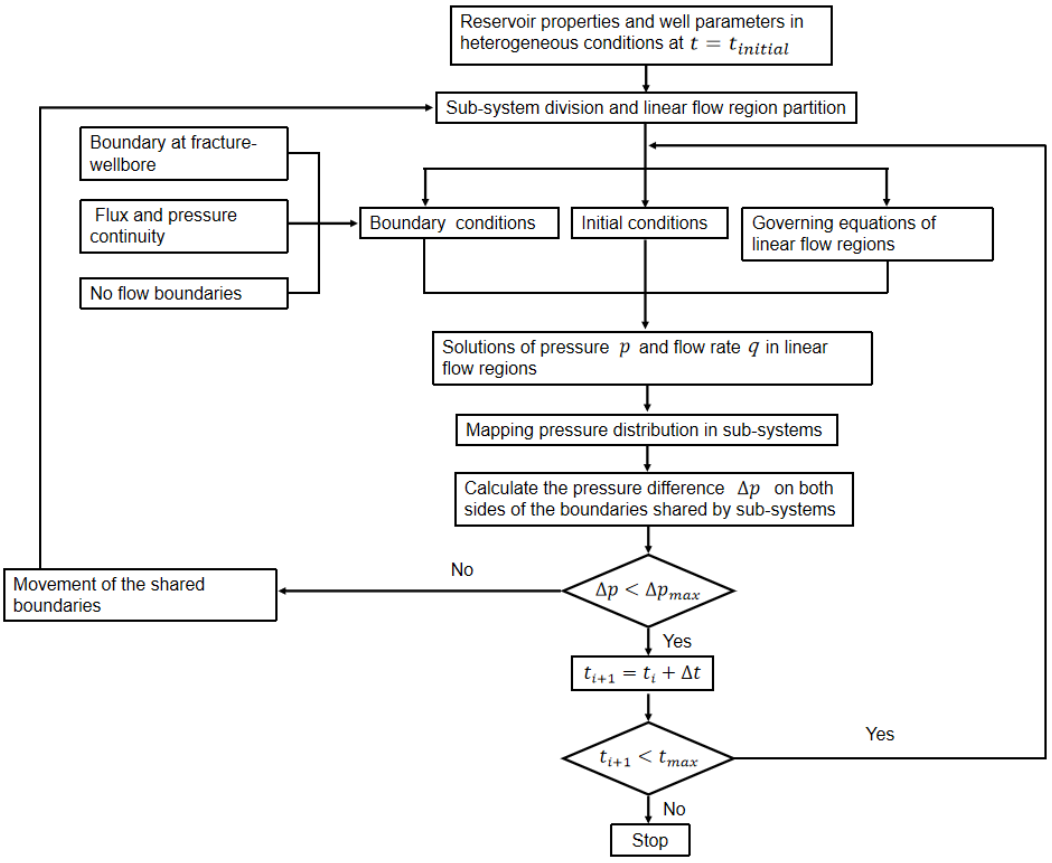

Figure 4. Flow Chart of the Semi-analytical Modeling for Fractured Horizontal Wells with Considering the Interferences between Hydraulic Fracture.

3. Model Verification

Our semi-analytical methodology can be utilized to simulate the variations of production rate vs. time and flowing bottomhole pressure vs. time for a given fractured horizontal well. This methodology is validated by the comparison with Five-region model (Stalgorova et al., 2013). Table 3 summarizes reservoir properties and well parameters used for the validation. Figure 5 displays that a 20-stage fractured horizontal well is located at the center of the reservoir. For each of the 20 hydraulic fractures, the part of the formation close to a hydraulic fracture has a permeability higher than the far-away region. Therefore, the reservoir can be divided into 20 equal sub-systems. All the boundaries among sub-systems remain static during the production, which enables the applicability of Five-region model in this heterogenous reservoir condition. Figure 6 compares the data of bottomhole flow pressure vs. time and their derivatives calculated with our semi-analytical model against the data calculated with Five-region model. The good agreement between the two sets of data validates that our semi-analytical methodology is applicable in simulating the fluid flow in a reservoir stimulated by fractured horizontal wells under heterogeneous conditions.

Table 3. Reservoir Properties and Wellbore Parameters in Model Verification.

Reservoir lateral length L	609.6 m
Well spacing W	304.8 m
Pay zone thickness H	30.48 m
Higher reservoir permeability k_1	1 mD
Lower reservoir permeability k_2	0.01 mD
High permeability region width x_1	7.62 m
Reservoir compressibility C_t	1.45×10^{-10} Pa^{-1}
Reservoir porosity ϕ	0.1
Viscosity μ	0.001 Pa·s
Dimensionless fracture conductivity F_{CD}	21.13
Fracture stages n	20
Fracture half-length x_f	30.48 m
Initial reservoir pressure p_i	68.9655 MPa
Production rate q	6.36 m^3/d

As shown in Figure 6, formation linear flow regime (I) lasts for a relatively short period (0.001, 0.02). The extent of the high-permeability region isn't long enough to support a longer-lasting formation linear flow regime. The interface between high-permeability and low-permeability regions works as a no-flow boundary for the fluid flow through the high-permeability region. Thus an "apparent" boundary dominated flow regime (II) occurs and lasts until $t_D = 200$. Before the final pseud-steady state (V) arrives, a short period of formation linear flow (III) contributed by the low-permeability region can be observed during the period of (200, 400). Flow regime IV is transition regime between formation linear flow and final pseud-steady state.

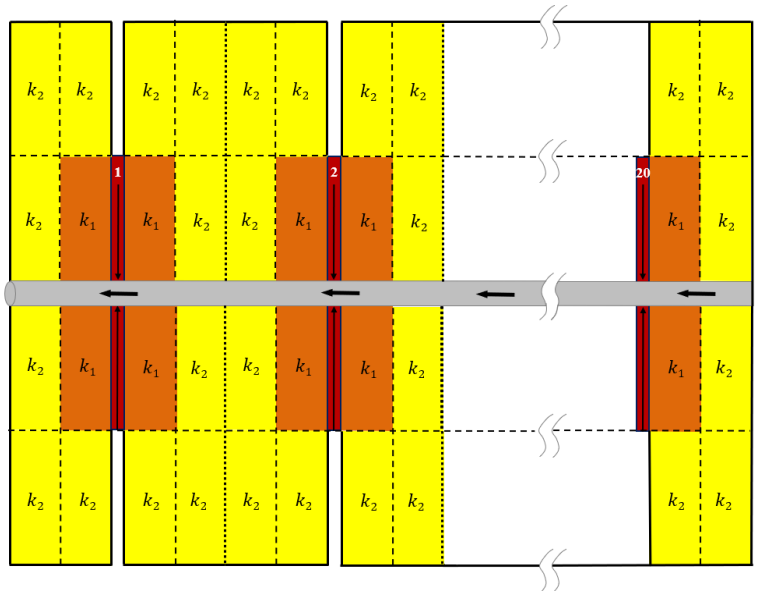

Figure 5. A 20-stage Fractured Horizontal Well Is Located at the Center of a Heterogenous Reservoir.

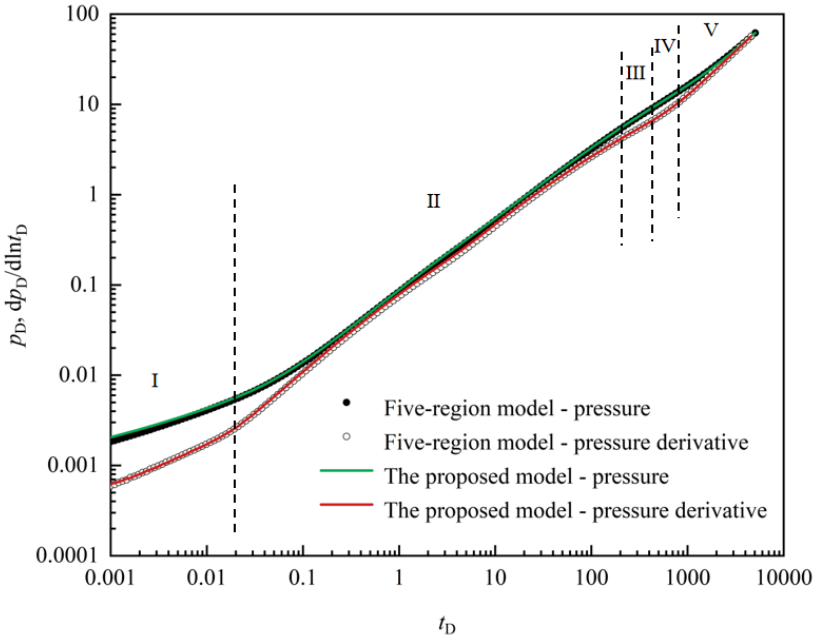

Figure 6. Comparsion of the Calculated Pressure vs. Time and Pressure Derivatives between the Proposed Semi-analytical Model and the Five-region Model (Stalgorova et al., 2013).

4. Model Application

This proposed model can be applied in complex heterogeneous conditions. A reservoir can be heterogenous in permeability and porosity through the extent of a horizontal wellbore. In addition, a horizontal well can exhibit a heterogeneous completion with fracture properties varying from stage to

stage. This section discusses the applicability of the proposed semi-analytical model in the two heterogeneous conditions. Reservoir properties and well parameters are same as those listed in Table 3 unless otherwise stated.

4.1 Heterogeneous Completions

Table 4. Reservoir Properties and Wellbore Parameters for a Fractured Horizontal Well with Heterogeneous Completions.

Reservoir lateral length L	60 m
Well spacing W	160 m
Pay zone thickness H	30 m
Reservoir permeability $k_1 = k_2$	0.1 mD
Low dimensionless fracture conductivity F_{CD1}	2
High dimensionless fracture conductivity F_{CD2}	20
Fracture stages n	2
Fracture half-length x_f	60 m

In many field scenarios, hydraulic fractures along a horizontal wellbore exhibit different fracture properties (Ambrose et al., 2011). The proposed model calculates the transient bottomhole pressures of a fractured horizontal well at constant production rate, while considering the interference between hydraulic fractures of distinct properties. In this section one set of reservoir properties and wellbore parameters is selected as shown in Table 4 and Figure 7. The horizontal well has a heterogeneous completion. As shown in Figure 7, No. 1 hydraulic fracture has a dimensionless conductivity much lower than No. 2 fracture.

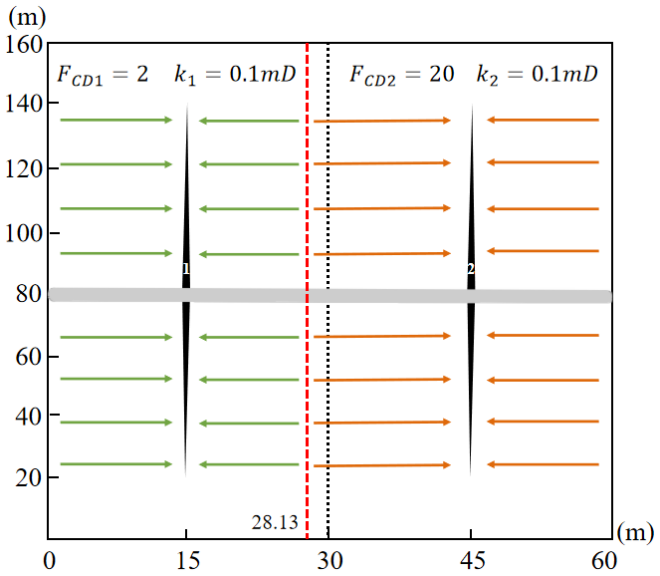

Figure 7. Interference between Adjacent Sub-systems for the Two-stage Fractured Horizontal Well with Heterogeneous Completion Listed in Table 4.

Figure 8 shows the data of flowing bottomhole pressure vs. time and pressure derivative vs. time calculated with our semi-analytical model for the horizontal well in Figure 7. Figure 8 suggests an extended formation linear flow regime followed by the pseudo-steady state flow. In this case the pseudo-steady state flow becomes evident once the interference between the two hydraulic fractures occurs. Our semi-analytical model develops two sub-systems according to the number of fracture stages. And the time when pseudo-steady state flow occurs is correlated to the minimum area among all the sub-systems. The semi-analytical modeling results suggest that the boundary shared by the two sub-systems controlled by each of the two fractures is located at 28.13 m when pseudo-steady state flow begins at $t_D = 8$. It supports that the formation area affected by No. 2 fracture of high conductivity is larger than that of No. 1 fracture.

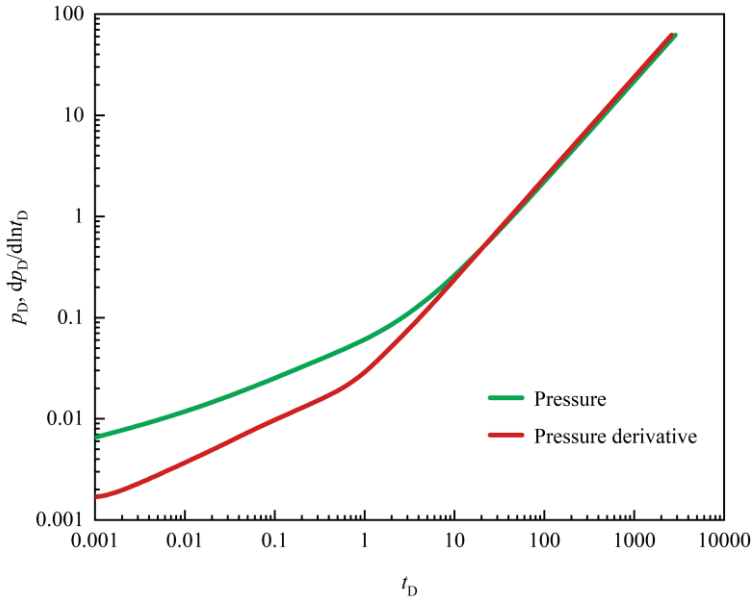

Figure 8. Variations of Pressure vs. time and Pressure Derivative vs. Time for a Fractured Horizontal Well with Heterogeneous Completion by the Proposed Model with Updated Boundaries.

4.2 Reservoir Heterogeneity along the Horizontal Wellbore

Table 5. Reservoir Properties and Wellbore Parameters for a Fractured Horizontal Well in a Heterogeneous Formation.

Reservoir lateral length L	60 m
Well spacing W	160 m
Pay zone thickness H	30 m
Dimensionless fracture conductivity $F_{CD1} = F_{CD2}$	20
Low reservoir permeability k_1	0.1 mD
High reservoir permeability k_2	1 mD

Fracture stages n	2
Fracture half-length x_f	60 m

Most of unconventional reservoirs exhibit different reservoir properties along the horizontal wellbore. In this section the proposed semi-analytical model is utilized to investigate the influence of such reservoir heterogeneity on fractured horizontal wells' production. One set of reservoir properties and wellbore parameters is selected for our simulation (Table 5). Reservoir properties and well parameters are same as those listed in Table 3 unless otherwise stated. Figure 9 provides a schematic of reservoir heterogeneity in permeability. The formation partition between (0 m, 30 m) is assigned a permeability of 0.1 mD while the other half of the formation has a much higher permeability of 1 mD.

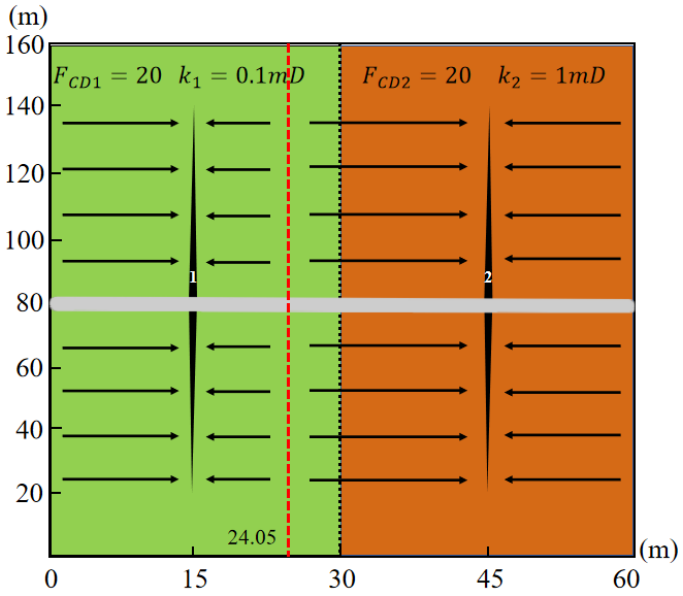

Figure 9. Interference between Adjacent Sub-systems for the Two-stage Fractured Horizontal Well in Heterogeneous Formation Listed in Table 5.

Figure 10 shows the data of flowing bottomhole pressure vs. time and pressure derivative vs. time calculated with our semi-analytical model for the horizontal well in Figure 9. Similar to Figure 8, the data in Figure 10 also supports an extend formation linear flow regime followed by the pseudo-steady state flow. Our semi-analytical model develops two sub-systems according to the number of fracture stages. The time when pseudo-steady state flow occurs depends on the minimum area among all the sub-systems. Figure 9 marks the location of the boundary shared by the two sub-systems at 24.05 m when the pseudo-steady state flow starts at $t_D = 4$. It demonstrates that the formation partition controlled by No. 2 hydraulic fracture reaches beyond the high-permeability region and therefore, owns a larger area than that controlled by No. 1 fracture. A part of low-permeability region provides linear flow towards the far-away second fracture rather than the first fracture.

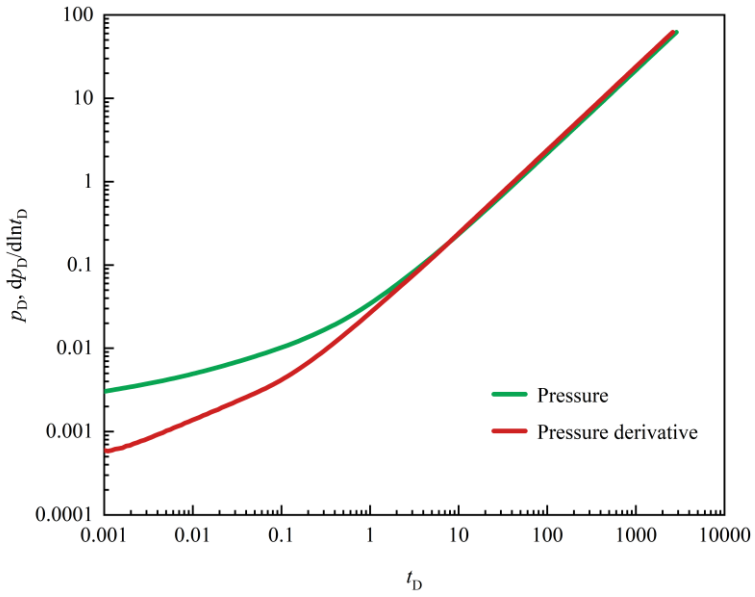

Figure 10. Variations of Pressure vs. Time and Pressure Derivative vs. Time for a Fractured Horizontal Well in Heterogeneous Reservoir by the Proposed Model with Updated Boundaries.

5. Field Example

The proposed model can generate type curves of production rate q vs. time t and flowing bottomhole pressure p_{wf} vs. time t. Fitting type curves to field data can provide estimation unknown reservoir and fracture properties. This section analyzes a set of production data from a gas field by using our semi-analytical model.

Data of gas production rate (under standard condition) Q_{sc} vs. t comes from a three-stage fractured horizontal well in a shale gas formation. The basic physical properties of the reservoir and fluid are given in Table 6. A 3-stage fractured horizontal well semi-analytical model is utilized for type curve matching. The proposed model has 3 sub-systems and all the sub-systems are assumed to be the same. Each sub-system is composed of x-direction linear flow regions, y-direction linear flow regions, and a hydraulic fracture region. In addition, porosity in all the regions (except hydraulic fracture region) is assumed to be the same. As shown in Figure 11, within a sub-system, linear flow regions near and away from the hydraulic fracture are given different reservoir permeability. Figure 12 shows the best-match scenario of our semi-analytical models as compared against the field production data. The best-match model supports that permeability k_1 of linear flow regions near the hydraulic fracture is 0.0008 mD while permeabilities k_2 and k_3 of the linear flow regions away from the hydraulic fracture are 0.0004 mD and 0.0002 mD, respectively. The fracture half-length and conductivity are selected to be 200 m and 5×10^{-16} m^3. Figure 13 provides the microseismic events of the well. There exist many microseismic events at each stage of the hydraulic fractures, implying the existence of secondary fractures around hydraulic fractures and therefore, a higher permeability in the vicinity of hydraulic fractures than the far-away regions.

Table 6. Reservoir Properties and Wellbore Parameters in the Field Case (Xu et al., 2015).

Reservoir lateral length L	1200 m
Pay zone thickness H	49 m
Reservoir temperature T	360 K
Reservoir porosity ϕ	0.001
Initial gas viscosity μ	0.022 Pa·s
Initial gas compressibility C_g	2.5×10^{-8} Pa^{-1}
Initial gas deviation factor Z	0.89
Fracture stages n	3
Initial reservoir pressure p_i	33.6 MPa
Bottomhole pressure p_{wf}	16 MPa

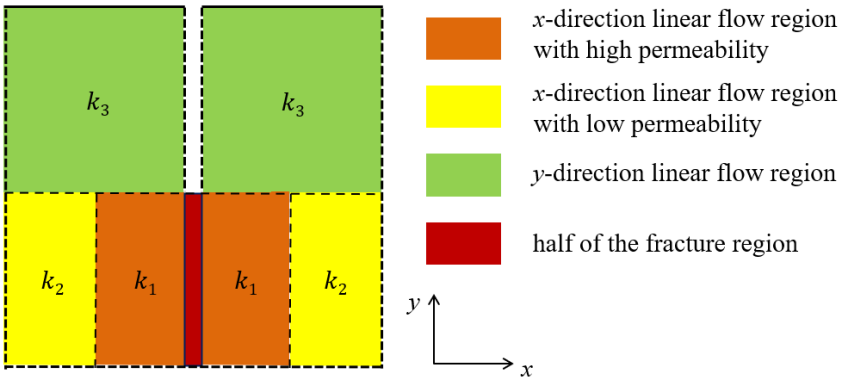

Figure 11. Linear Flow Regions in the Vicinity of Hydraulic Fracture Have Permeability Different from That of the Regions Far from the Fracture.

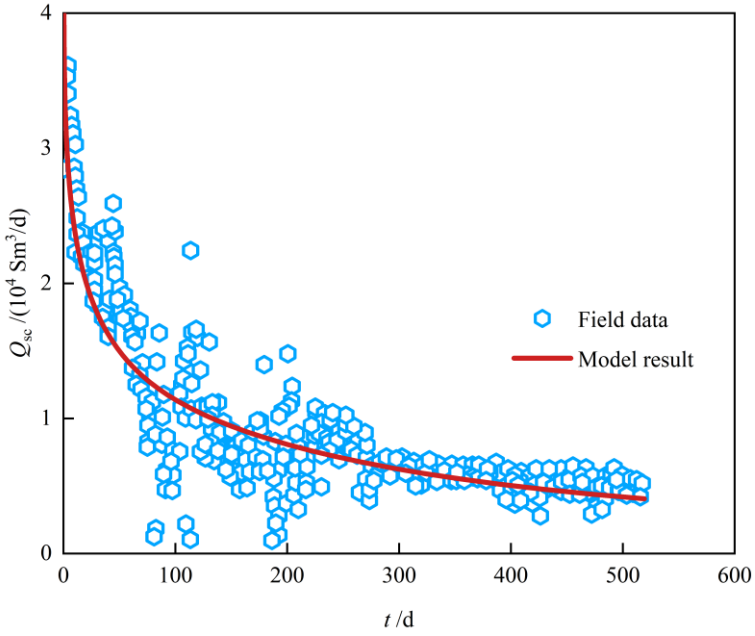

Figure 12. Comparison of the Field Data with the Results Obtained from the Proposed Model.

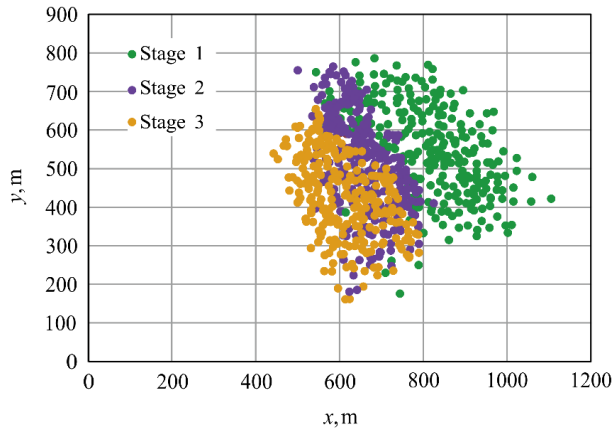

Figure 13. Microseismic Events of the Well (Xu et al., 2015).

6. Conclusions

In addressing the complex flow problem caused by multi-stage fracturing treatments in heterogeneous conditions, this paper establishes a semi-analytical well testing model for multi-stage fractured horizontal wells.

(1) In simulation of the flow of fluid in fractured horizontal wells, the proposed mode, based on the assumption of linear flow, extends linear flow models in literature with considering the distribution characteristics of pressure in heterogeneous reservoirs and quantifying the interference between hydraulic fractures.

(2) The proposed model is validated and applicable to complex heterogeneous reservoirs, including heterogeneous completions and reservoir heterogeneity around the horizontal well. Fluid flow modeling by using this proposed semi-analytical methodology proves that the interference of hydraulic fractures can lead to the movement of boundaries between sub-systems especially under heterogeneous conditions.

(3) Matching type curves from the proposed model with production data can well estimate the properties of underground reservoir and hydraulic fractures, including reservoir permeability, hydraulic fracture half-length and fracture conductivity.

Nomenclature			
B_o	formation volume factor for oil, dimensionless	s	Laplace parameter
B_g	formation volume factor for gas, dimensionless	w_f	fracture width, m
μ	fluid viscosity, Pa·s	x_f	fracture half-length, m
ϕ	porosity, fraction	x	distance in the *x*-direction, m
k	permeability, m^2	y	distance in the *y*-direction, m
C_t	total compressibility, Pa^{-1}	η	diffusivity, m^2/s
p	pressure, Pa	L	horizontal wellbore length, m
$\bar{p}$	pressure in Laplace domain, Pa	W	well spacing, m
p_{wf}	bottomhole flowing pressure, Pa	H	pay-zone thickness, m
q	flow rate, m^3/s	*Subscripts*	
$\bar{q}$	flow rate in Laplace domain, m^3/s	D	dimensionless
t	time, s	ref	reference
		f, F	hydraulic fracture

References

Ambrose, R.J., Clarkson, C.R., Youngblood, J., et al. (2011). Life-Cycle Decline Curve Estimation for Tight/Shale Reservoirs. Paper SPE 140519, presented at the SPE Hydraulic Fracturing Technology Conference and Exhibition held in The Woodlands, Texas, USA, 24-26 January, 2011. https://doi.org/10.2118/140519-MS

Brown, M., Ozkan, E., Raghavan, R., et al. (2011). Practical Solutions for Pressure-Transient Responses of Fractured Horizontal Wells in Unconventional Shale Reservoirs. *SPE Reservoir & Evaluation*, *14*(6), 663-676. https://doi.org/10.2118/125043-PA

Cinco-Ley, H., Samaniego-V, F. (1981). Transient Pressure Analysis for Fractured Wells. *Journal of Petroleum Technology*, *33*(9), 1749-1766. https://doi.org/10.2118/7490-PA

Deng, Y., Fan, C., Hu, D., et al. (2023). Heterogeneity of Shale Oil Reservoirs in the $E_2l^{2(1)}$ in Weixinan Sag, Beibu Gulf Basin. *Oil & Gas Geology*, *44*(4), 923-936.

Denney, D. (2010). Thirty Years of Gas-Shale Fracturing: What have we learned? *Journal of Petroleum Technology*, *62*(11), 88-90. https://doi.org/10.2118/1110-0088-JPT

Freeman, C.M., Moridis, G., Ilk, D., et al. (2013). A Numerical Study of Performance for Tight Gas and Shale Gas Reservoir Systems. *Journal of Petroleum Science and Engineering*, *108*, 22-39. https://doi.org/10.1016/j.petrol.2013.05.007

Grieser, B., Shelley, B., Soliman, M. (2009). Predicting Production Outcome from Multi-stage, Horizontal Barnett Completions. Paper SPE 120271, presented at the 2009 SPE Production and Operations Symposium held in Oklahoma City, Oklahoma. USA, 4-8 April, 2009. https://doi.org/10.2118/120271-MS

King, G.E. (2014). 60 Years of Multi-fractured Vertical, Deviated and Horizontal Wells: What Have We Learned? Paper SPE-170952-MS, presented at the SPE Annual Technical Conference and

Exhibition held in Amsterdam, The Netherlands, 27-29 October, 2014. https://doi.org/10.2118/170952-MS

Lee, S.T., Brockenbrough, J.R. (1986). A New Approximate Analytic Solution for Finite-Conductivity Vertical Fractures. *SPE Formation Evaluation*, *1*(1), 75-88. https://doi.org/10.2118/12013-PA

Ning, B., Xiang, Z., Liu, X., et al. (2020). Production Prediction Method of Horizontal Wells in Tight Gas Reservoirs Considering Threshold Pressure Gradient and Stress sensitivity. *Journal of Petroleum Science and Engineering*, *187*, 106750. https://doi.org/10.1016/j.petrol.2019.106750

Nobakht, M., Clarkson, C.R. (2012). A New Analytical Method for Analyzing Linear Flow in Tight/Shale Gas Reservoirs: Constant-Flowing-Pressure Boundary Condition. *SPE Reservoir Evaluation & Engineering*, *15*(3), 370-384.

Ren, J. Guo, P., Guo, Z., et al. (2014). A Lattice Boltzmann Model for Simulating Gas Flow in Kerogen Pores. *Transport in Porous Media*, *106*(2), 285-301. https://doi.org/10.1007/s11242-014-0401-9

Seales, M.B. (2020). Multiphase Flow in Highly Fractured Shale Gas Reservoirs: Review of Fundamental Concepts for Numerical Simulation. *Journal of Energy Resource Technology*, *142*(10), 100801. https://doi.org/10.1115/1.4046792

Song, B., Ehlig-Economides, C. (2011). Rate-normalized Pressure Analysis for Determination of Shale Gas Well Performance. Paper SPE 144031, presented at the SPE North American Unconventional Gas Conference and Exhibition held in The Woodlands, Texas, USA, 14-16 June, 2011. https://doi.org/10.2118/144031-MS

Stalgorova, E., Mattar, L. (2013). Analytical Model for Unconventional Multifractured Composite Systems. *SPE Reservoir & Evaluation*, *16*(3), 246-256. https://doi.org/10.2118/162516-PA

Wang, W., Su, Y., Sheng, G., et al. (2015). A mathematical Model Considering Complex Fractures and Fractal Flow for Pressure Transient Analysis of Fractured Horizontal Wells in Unconventional Reservoirs. *Journal of Natural Gas Science and Engineering*, *23*, 139-147.

Wei, Y., He, D., Wang, J., et al. (2015). A Coupled Model for Fractured Shale Reservoirs with Characteristics of Continuum Medium and Fractal Geometry. Paper SPE-176843-MS, presented at the SPE Asia Pacific Unconventional Resources Conference and Exhibition held in Brisbane, Australia. 9-11 November, 2015. https://doi.org/10.2118/176843-MS

Xie, Y., He, Y., Hu, Y. et al. (2022). Study on Productivity Prediction of Multi-stage Fractured Horizontal Well in Low-permeability Reservoir Based on Finite Element Method. *Transport in Porous Media*, *141*(3), 629-648. https://doi.org/10.1007/s11242-021-01739-3

Xu, J., Guo, C., Wei, M., et al. (2015). Production Performance Analysis for Composite Shale Gas Reservoir Considering Multiple Transport Mechanisms. *Journal of Natural Gas Science and Engineering*, *26*, 382-395. https://doi.org/10.1016/j.jngse.2015.05.033

Yao, S., Wang, X., Yuan, Q., et al. (2020). Production Analysis of Multifractured Horizontal Wells with Composite Models: Influence of Complex Heterogeneity. *Journal of Hydrology*, *583*, 124542. https://doi.org/10.1016/j.jhydrol.2020.124542

Yao, S., Zeng, F., Liu, H., et al. (2013). A Semi-analytical Model for Multi-stage Fractured Horizontal Wells. *Journal of Hydrology*, *507*, 201-212. https://doi.org/10.1016/j.jhydrol.2013.10.033

Yuan, B., Su, Y., Moghanloo, R.G., et al. (2015). A New Analytical Multi-linear Solution for Gas Flow toward Fractured Horizontal Wells with Different Fracture Intensity. *Journal of Natural Gas Science and Engineering*, *23*, 227-238.

Yuan, J. (2023). New Progress and Development Proposal of Sinopec's Drilling Technologies for Ultra-Long Horizontal Shale Gas Wells. *Petroleum Drilling Techniques*, *51*(4), 81-87.

Yue, M., Leung, J., Dehghanpour, H. (2013). Integration of Numerical Simulations for Uncertainty Analysis of Transient Flow Responses in Heterogeneous Tight Reservoirs. Paper SPE 167174, presented at the SPE Unconventional Resources Conference-Canada held in Calgary, Alberta, Canada, 5-7 November. https://doi.org/10.2118/167174-MS

Zawila, J., Fluckiger, S., Hughes, G., et al. (2015). An Integrated, Multi-disciplinary Approach Utilizing Stratigraphy, Petrophysics, and Geophysics to Predict Reservoir Properties of Tight Unconventional Sandstones in the Powder River Basin, Wyoming, USA. Paper presented at New Orleans Annual Meeting, 2015.

Zeng, J., Wang, X., Guo, J., et al. (2018). Composite Linear Flow Model for Multi-fractured Horizontal Wells in Tight Sand Reservoirs with the Threshold Pressure Gradient. *Journal of Petroleum Science and Engineering*, *165*, 890-912. https://doi.org/10.1016/j.petrol.2017.12.095